In: Nelson, Gordon L., ed. Fire and polymers II. Materials and tests for hazard prevention: Proceedings of 208th National meeting of the American Chemical Society; 1994 August 21-26; Washington, DC. ACS symposium series 599. Washington, DC: American Chemical Society, 1995. Chapter 29.

Chapter 29

Protocol for Ignitability, Lateral Flame Spread, and Heat Release Rate Using Lift Apparatus

Mark A. Dietenberger

Forest Service, Forest Products Laboratory, U.S. Department of Agriculture, One Gifford Pinchot Drive, Madison, WI 53705-2398

In this study, protocols in ASTM E 1321 for determining piloted ignition and flame spread properties and in E 1317 for deriving heat release rate are modified to improve generality, accuracy, and efficiency. We report on new methods that improve the calibration of radiative and convective heat flux profiles on the exposed material, such as Douglas Fir plywood. A simple direct measure of surface emissivity completes the boundary conditions for material thermal analysis. A crank-operated indicator, interfaced with data acquisition system, tracks the lateral flame front to the spread of flame limit. Features of our lateral flamespread model include a range of preheating the sample before flame spreading, the transitioning from thick to thin thermal behavior, and a limit to flame spread. Cur improvement to E 1317 in measuring heat release rate profile is demonstrated.

Our initial intention was to implement ASTM E-1321 *(1)* and E-1317 *(2)* protocols and use these standards to obtain material and flammability properties for wood products. Specifically, the Forest Products Laboratory (FPL) wanted to assess ignitability of exterior siding materials and interior panels. Also, thermophysical material properties were needed for use in room fire growth models. Despite substantial progress made in understanding and measuring ignitability and creeping flame spread, inconsistencies remained between the various bench-scale tire tests and their suitability to derive thermophysical properties of test samples. Even with the Cone Calorimeter (ISO 5660, *(3))*. one finds great variation in time to ignition near the critical irradiance (which also varies greatly *(4))* when effects of geometry and ignition mode are investigated *(5)*. As a result of trying to implement E 1321, we needed to remedy deficiencies in calibrations of burner irradiances and convective heat transfer coefficients and in modeling piloted ignition. These are discussed in the ignitability section. Measurement and modeling of lateral flame spread also needed improvement, because test derived thermophysical constants were not consistent with those derived from

This chapter not subject to U.S. copyright
Published 1995 American Chemical Society

ignitability analysis, and changes in certain thermal behaviors during flame spreading were not accounted for in E 1321. These are addressed in the lateral flame spread section.

ASTM E-1317 provides a thermopile method to measure the heat release rate of a spreading lateral fire on the 150- by 800-mm specimen sample for a fixed panel burner setting. The Lateral Ignition and Flame-spread Test (LIFT) apparatus employed by ASTM E-1317 and E-1321 is not as accurate as the Cone Calorimeter for measuring heat release rates on a small square specimen because oxygen consumption calorimetry is not used in LIFT. However, with flame spreading on the larger specimen, the measurement of total heat and mass release is useful in validation of a fire growth model. Upon further investigation, we determined that improvement to the thermopile method for the LIFT apparatus could be made. As a result, new procedures to calibrate the heat release rate measurements and correlate heat release rate with the thermopile, compensator thermocouple, and pyrometer measurements are discussed in the heat release rate section.

Ignitability

Piloted ignition is difficult to assess for composite materials such as wood products. By using a finite difference model (FDM), Janssens *(6)* shows there is a transition behavior from thermally thick to thin as the ignition time gets very large. If the material also has a broad range of surface temperature in which char develops, such as wood, surface emissivity and temperature at ignition may deviate significantly so that the critical heat flux is elusive to measure. In his work with wood products tested in the Cone Calorimeter, Janssens suggested nominal values for the surface emissivity and convective heat transfer coefficient in analogy with the protocol described for the LIFT apparatus. We examined these physical processes in depth for the LIFT apparatus and found an alternative, more accurate approach for deriving thermophysical properties using Douglas Fir plywood as an example.

Calibrations. First, we calibrated the irradiance profile on the specimen by using a linear relationship between panel-burner heat-fluxes measured by the pyrometer and the water-cooled fluxmeters. These fluxmeters were inserted flush with the exposed surface and laterally every 100-mm along the 150- by 800-mm calibration board which is orientated 15 degrees laterally away from the panel-burner. The specimen holder was aligned such that the irradiance profile was within the limits required by E 1321. Nonlinearity between these two fluxes near the hot end of the specimen occurs because of (1) convective and radiative heat losses from the fluxmeters at ambient temperatures other than the optimum value of T_a **= 26 °C,** (2) flame impingement on the sample at high burner irradiances, and (3) orange-colored flames resulting from excessive carbon deposits on the burner grid. Thus, it has become our practice prior to testing to ramp slowly (in at least 10 minutes) the LIFT panel burner to the maximum and back to a minimum value while recording the signals from the pyrometer and at least two fluxmeters (The first at 50-mm location and the second at 350-mm location.). Then, these linear relationships are checked against the original calibration before proceeding

with the daily testing. To better define the specimen's irradiance, we normalized its profile with respect to the pyrometer's irradiance rather than with respect to the fluxmeter at the 50-mm location as specified in E 1321.

Second, the convective heat transfer coefficient was calibrated for our LIFT apparatus. Since the values for convective heat flux were needed in an intermediate step, accurate values for the difference of net radiative heat flux and specimen's surface conductive flux were obtained. In addition to the panel irradiance profile already calibrated, the surface emissivity and temperature needed to be measured to derive the net radiative surface heat flux. The value for the surface conductive heat flux is obtained from the product of material thermal conductivity and temperature gradient at the surface. To maximize the convective heat losses and obtain fairly large temperature gradient in the material, we used insulative plugs inserted in place of the fluxmeters. These plugs were the same insulative material as the board holding the fluxmeters and the plugs, so that with our low-cost emmisometer we could directly measure the surface hemispherical emittance. Three thermocouples were inserted at fixed depths within the plugs and an interpolation function was used to derive the surface temperature and its gradient. Long before the temperatures reached steady-state during exposure to selected irradiances, the material conductive heat flux became small compared with other terms, and the derived convective heat transfer coefficient, h_c (convective heat flux over surface temperature rise) became constant.

The E-1321 recommendation of 0.015 kW/Km^2 for h_c was investigated using quite different assumptions than those in the previous paragraph. Surface emissivity, ε_s, was assumed to be unity. An FDM code together with a surface thermocouple were used to derive the surface conductive heat flux. Burner irradiance was equated to that measured with a water-cooled fluxmeter. The reported measurements seem limited to locations within 250 to 600 mm and at a flux of 50.5 kW/m^2 at the 50-mm location. There was a need to consider full lateral length of specimen, full range of panel burner irradiance, and full range of methane calibration burner.

Figure 1 shows the result using our method of deriving h_c and shows measurements for 50-, 350-, and 650-mm positions, for panel irradiances at 50 mm of about 22, 37, 51, and 71 kW/m^2. The derived values of h_c are much greater than can be expected from the air flow induced by the heated specimen (6). In Figure 1, data correlate best with one-fourth power of the panel irradiance, I_{50}, which suggests that the gas panel burner induce air flow over the specimen; h_c also has a significant linear decrease with lateral distance from the hot end,

$$h_c = (0.0139 - 0.0138x)\, I_{50}^{1/4} \quad kW/Km^2 \qquad (1)$$

that may be expected with a turbulent air flow within an angled wedge. The methane calibration T burner coveted the lateral positions from 100 to 300 mm so that it was between two instrumented plugs. The objective was to see if flaming from the specimen location has an effect on h_c derived at instrumented plug locations. The results show specimen flaming has nil effect on h_c. This systematic study of the

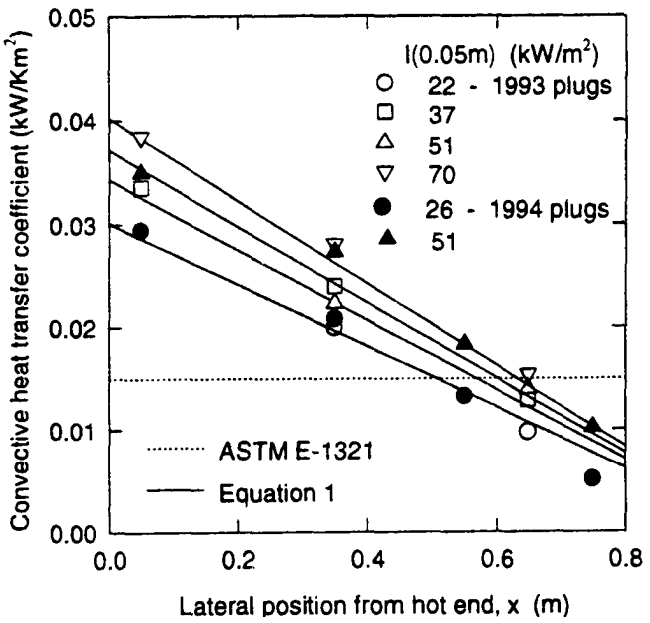

Figure 1 Correlation of convective heat transfer coefficient on specimen holder

convective heat transfer coefficient suggests that the value recommended by E-1321 is severely in error and should be replaced by a procedure to calibrate the convective heat transfer coefficient as outlined in this section.

Douglas Fir Plywood Example. The times to ignition of Douglas Fir plywood with varying thicknesses (**6** to 15 mm) were measured over the full range of the gas panel irradiances up to 70 kW/m^2. The plywood samples were prepared in the test lab, where conditions were about 30% relative humidity and 23°C. Emissivity measured an average of 0.86. For ignition time less than 30 seconds, a flip-out aluminum sheet was used to protect the specimen until the initiation of the test. Data obtained were initially plotted as time to ignition, t_{ig}, raised to the -0.547 power as function of irradiance following Janssens (6) recommendation. The thin plywood (6.55 mm and 12.7 mm) did not correlate well with the recommended straight line and had the largest disagreement near the critical flux level, q_{ig}, which corresponds to an infinite ignition time. With a finite difference analysis, Janssens shows a theoretical basis for this bias to be the transition behavior from thermally thick to thin for finitely thick materials. As an added difficulty, criteria for the transition use thermal properties not generally available. To remedy this situation, formulas based on our extensive finite element model solutions were developed for materials of finite thickness which was cooled connectively and radiatively on the exposed side and insulated on the unexposed side. Most accurate is the interpolation between thermally thick and thermally thin correlations with an adjustment factor including the Biot number, ***Bi,*** and Fourier

number, Fo, as follows:

$$\frac{q_{ig}}{q_e} = T = \left(T_{thick}^{5} + \frac{T_{thin}^{5}}{1 + 0.574\, Bi^{1.31}} \right)^{1/5} \tag{2}$$

where

$$T_{thick} = 1 / \left(1 + 0.73\, (Bi^2 Fo)^{-0.547} \right) \tag{3}$$

$$T_{thin} = 1 - \exp(-Bi\, Fo) \tag{4}$$

$$Fo = \alpha\, t_{ig} / \delta^2 \tag{5}$$

$$Bi = h_{ig}\, \delta / \lambda \tag{6}$$

$$h_{ig} = h_c + \varepsilon_s\, \sigma (T_{ig}^2 + T_a^2)(T_{ig} + T_a) \tag{7}$$

$$q_{ig} = h_{ig}\, (T_{ig} - T_a) / \varepsilon_s \tag{8}$$

In examining equations 2 to 8, we note that material thickness, δ, should be measured in addition to the usual values of ε_s, h_c, I_{50}, t_{ig}, and T_a. There are three fitting parameters: surface temperature at ignition, T_{ig}, thermal diffusivity, α, and thermal conductivity, λ. In a test series, the variation of a step-function irradiance with time to ignition is measured. This is shown in Figure 2 for three different thicknesses of Douglas Fir plywood along with the curves given by the predicted irradiance, $q_e = q_{ig} / T$, fitted to the pyrometer measured values, I_{50}. Values of fitting parameters are T_{ig} = 608.2 K (a typical pyrolysis temperature of wood), $\alpha = 1.48 \times 10^{-7}$ m^2/s (a known value for thermal diffusivity of Douglas Fir wood *(6))*, and λ = 0.164 W/km. Corresponding parameters also have the values q_{ig} = **17 kW/m^2**, h_{ig} = ***0.048*** kW/Km^2, and ρC_p = 1108 kJ/Km^3.

Further examination of Figure 2 shows the effect that improving the functional correlations has on fitting the ignitability data. Janssens *(6)* demonstrated that the correlation used in the E-1321, seen with dot-dashed line legend in Figure 2, is strictly valid only where q_{ig}, given by the dotted line, is less than 30% of q_e. This means fluxes greater than 59 kW/m^2, instead of all data as recommended in E 1321, should only be used to determine the parameter, b, in the correlation. The result is the dot-

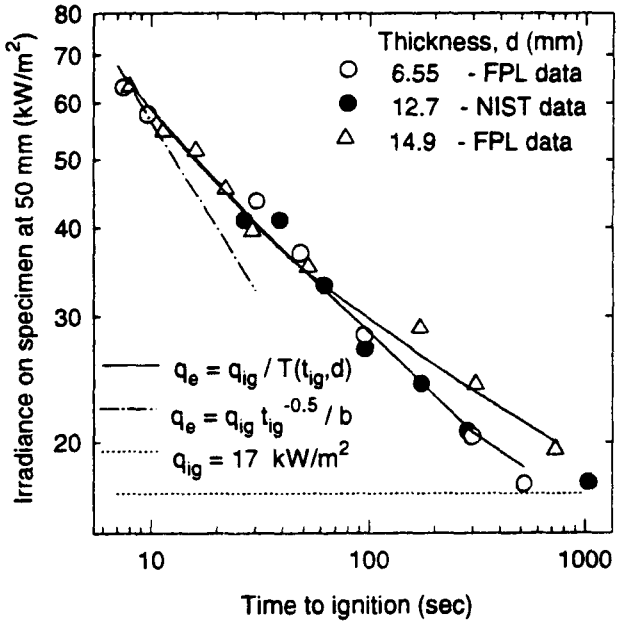

Figure 2 Correlation of irradiance versus time to ignition of Douglas Fir plywood

dashed line with b = 0.095. To validly incorporate more data, Janssens suggested using $q_e = q_{ig}/T_{thick}$ in the regime where the material is known to be thermally thick (upper solid curve in Figure 2). Thus, for the example of our 6.55-mm-thick plywood, this thermally thick regime is greater than 35 kW/m^2, just as the curves of equation 2 fan-out in Figure 2. In simpler correlations, the thermal diffusivity and conductivity could not be determined separately as can now be done with equation 2.

To clarify inconsistent critical heat flux values in recent studies of ignitability, let's take a value, h_c = 0.0135 kW/m^{2}K, recommended by Janssens *(6)* for the Cone Calorimeter. Using this value and the calibrated values of emissivity and ignition temperature for Douglas Fir plywood in equations 7 and 8, the critical irradiance is computed as 12.1 kW/m^2. This is 5 kW/m^2 less than that for our LIFT apparatus! Thus, differing apparatus provide correct but differing critical fluxes and need a correction factor to extrapolate to other geometries.

Lateral Flame Spread

Since creeping flame spread can be an integral feature of a fire growth model, such as the furniture fire model *(7)*, one tries to use flame spread properties derived from a flame spread apparatus, such as the LIFT. E-1321 prescribes flame front viewing rakes with pins spaced 50 mm apart. A pair of rakes, as observed through a floor level mirror, is used to line up pairs of pins to locations on the specimen. As the flame front reaches a lined-up pair of pins the observer writes down the time of

occurrence. To derive flame spread properties for the model described in ASTM E-1321, the material sample is required to be heated to steady-state before igniting to get lateral flame spread. This preheating often causes surface properties to change significantly (such as charring on wood) and results in a lateral surface temperature profile not anticipated by the model. In addition, the imposed heat flux at ignition location is limited to 5 kW/m^2 above critical flux, because premature ignition can occur at greater fluxes before the material temperature teaches steady state, and flame spread rates need to be slow enough for manual observation and recording.

FPL Method. Our alternative indicator of the flame front position is a pair of pins perpendicular to each other mounted on a movable platform driven by a crank-operated, 1-m-long shaft brass screw. The shaft is connected to a potentiometer so that the lateral position of the movable platform is converted to millivolt signals. The operator cranks the device handle to keep the pair of pins in alignment with the flame front. The floor mirror is used so that the pins can be located away from the flame so as not to disturb the flame With our data acquisition system, we can obtain data at short time intervals. This allows us to capture the initial high rates of flame spread and rapid decreases to low flame spread velocities. In addition, the spread of flame limit can be accurately pinpointed. Measuring the arrival times at 50-mm increments and performing a numerical differentiation to obtain the flame spread velocities causes significant errors during the initial rapid spread and near the spread of flame limit. Using the movable indicator should improve the required resolution.

This method of measuring creeping flame spread will likely show the limitations with simple correlations for flame spreading rate. A formula developed by Dietenberger *(8)* shows certain physical features such as (1) the transition from thermally thick to thermally thin behavior, both in preheat temperature and the flame spreading rate; (2) the transition from convective cooling by the induced airflow to convective heating from the flame edge; and (3) the transition to spread of flame limit at some minimum flux below the critical flux. This single formula was successfully applied to many existing creeping flame spread data for polymethylmethacrylate and paper and is simplified for Douglas Fir plywood to result in the following:

$$V_f = V_{f\infty}\left(\frac{1}{2} + \sqrt{\frac{1}{4} + (\delta^*/\delta)^{1.3}}\right)^{\frac{2}{1.3}} \tag{9}$$

$$V_{f\infty} = \frac{\delta_f}{\rho C_p \lambda}\left(\frac{q_{cf}}{T_{ig} - T_e} - (h_{ig} - h_c)\right)^2 \tag{10}$$

$$\delta^* = \lambda\left(\frac{q_{cf}}{T_{ig} - T_e} - (h_{ig} - h_c)\right)^{-1} \tag{11}$$

$$\delta_f = 2\,\lambda_a / \rho_a C_{pa} V_a \tag{12}$$

$$q_{cf} = \sqrt{2}\,\lambda_a (T_f - T_{ig}) / \delta_f \tag{13}$$

$$V_a = V_f + \sqrt{2C(T_f/T_a - 1)\,g\,\delta_f} \tag{14}$$

The preheat temperature, T_o, is substituted for ignition temperature, T_{ig}, in equation 8 and is where the panel irradiance and convective cooling profiles affect the flame spread behavior as a function of time-to-ignition. The convective heat flux from the flame edge has the magnitude, q_{cf} at the point of ignition and an exponential surface decay length of δ_f. Since the point of ignition moves at the flame spreading rate, V_f, the surface distance traveled was converted to the time domain so that the Laplace transform solution of the thermal diffusion equation predicts the surface temperature rise from preheat value to ignition value as a function of flame spreading velocity. A convenient interpolation between the exact thermally thick and thin solutions similar to equation 2 was rearranged to result in equations 9 to 11. Note that if the preheat temperature is low enough, then equation 10 approaches zero as a result of adjusted surface radiant flux equating to flame edge heat-flux. In addition, equation 11 will approach a large value, causing a thermally thin spreading behavior for equation 9. On the other hand, if the preheat temperature approaches ignition temperature, the flame spread rate will approach infinity and is the basis for piloted ignitability. Equations 12 to 14 were used because they represent creeping flame spread by the deRis solution and provide additional information about the flame edge. Finally, a better comparison with the data cart be achieved by numerically integrating the predicted flame spread rate and plotting the result with the experimental flame position as a function of time. We did this for Douglas Fir plywood.

Flame Spread on Douglas Fir Plywood. Figure 3 shows the lateral position of the flame front in the application of our movable flame spread indicator. Minimal preheating, just enough to ignite the plywood on the hot end within a few seconds, was applied. The solid curve in Figure 3 is the numerical integration of the flame spread velocity given by equation 9 and with the constants C = 1.3 and T_f **= 1234 K.** Substituting these constants into equations 12 to 14, we obtain q_{cf} **= 80** kW/m^2 and δ_f = 0.29 mm, which are reasonable. In Figure 3, four phases of lateral flame spread are represented. The first phase is characterized by initial rapid flame spread and decelerating rapidly as a result of the preheated temperature profile. Recall that the preheated temperature is affected significantly both by irradiance and convective cooling. In the next phase, a strip fire separates from the primary fire because an irradiance below a minimum level (about 13 kW/m^2 at the 370 mm location) is reached by which a heavily charred wood surface does not sustain burning. The third phase occurs at 200 seconds, when preheated temperature transitions to thermally thin

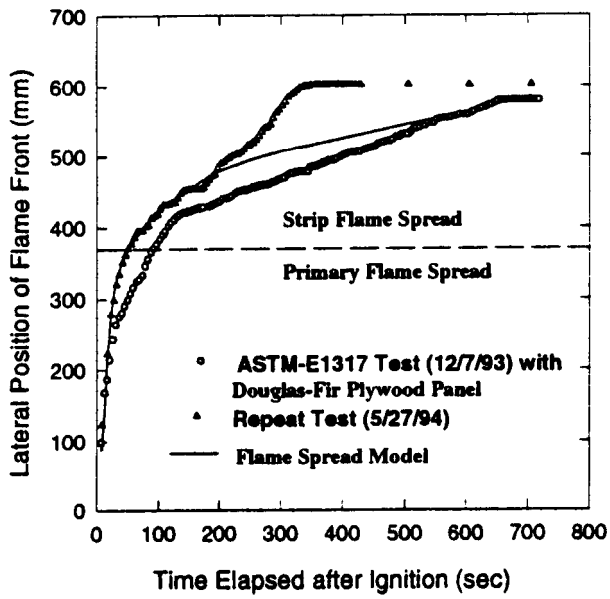

Figure 3 Flame spread data using new indicator and comparison with formula

behavior as it approaches equilibrium temperature. The final fourth phase occurs when flame spread rate transitions to a thermally thin behavior right near spread of flame limit (irradiance of 3.2 kW/m^2 at 580-mm position). Our repeat test of flame spread shown in Figure 3 deviates significantly from that of the initial test at long ignition times. Thus, uniformity and conditioning of the test material needs improvement.

Rate of Heat Release

Beyond construction details of E-1321, E-1317 describes the construction of the fume stack and the locations of the thermopile and compensator thermocouple on the stack. The idea is to sense the temperature rise of the air exiting the fume stack caused by flaming of the specimen and to convert the signals to calculations of the heat release rate. The purpose of E-1317 **is** to provide flammability ratings using the irradiance at 50 mm set at 50.5 kW/m^2. The flame front position and the heat release rate are measured as a function of time. This information is processed into different representations that suggest levels of flammability for the material. To gain additional information, we installed a fluxmeter about 40 mm below the compensator thermocouple on the fume stack.

For our methane calibration burner, we first used the E-1317 design. It prescribes a 2-m-length tube with holes near the hot end and was placed in the middle of the calibration holder. However, the tube covered our previously mentioned instrumented plugs and stuck precariously out from the apparatus. As a more

convenient, but equivalent design, we modified the ASTM E-906 methane "T" calibration burner and attached it to a portable stand so that the burner head was located directly on the calibration holder.

The approach described in E-1317 for calibrating the heat release rate measurement is typical when using the thermopile method. As a first step, a fraction of the compensator signal is subtracted from the thermopile signal to arrive at ***a*** signal that is approximately a square wave as the calibration burner is flaming and then shut off. This correction to the thermopile signal is usually needed because of the thermal inertia of the fume stack. In the next step, the panel irradiance is set at 50.5 kW/m^2, and the methane gas flow rate through the burner is incremented and measured as the burner is flaming. This measured flow rate is converted to heat release rates using the heat of combustion for methane gas and is correlated with the "corrected" thermopile's signal. We examined the basis of this approach.

FPL Modifications. Our results with the fluxmeter show that the total heat flux from the heated air in the fume stack to the water-cooled fluxmeter is solely a power function of the thermopile temperature-rise above ambient. This striking correlation was also found to apply at other panel irradiance settings to a good approximation. Thus, the heat transfer coefficient is proportional to the thermopile temperature-rise raised to the 0.65 power. Since the convective heat transfer coefficient primarily varies as a function of the air mass flow rate near the exit of the fume stack, the air mass flow rate is then only a function of the thermopile temperature. Since the enthalpy heat rate of exiting air is the product of the mass flow rate and the temperature-rise, it is therefore only a function of the thermopile temperature rise. Examination of the ratio of fume stack temperature-rise to thermopile temperature-rise showed that it has a steady state value around 0.645, independent of the methane burner or panel irradiance setting. However, during the transient phase (when the methane burner is lit or turned off), the compensator lags behind the thermopile because of the heat capacitance of the fume stack. This means that the steady-state heat-loss to the fume stack is proportional to the heat flux on the water-cooled fluxmeter installed on the fume stack. Therefore, the steady heat loss rate from the fume stack to surroundings is ultimately only a power function of the thermopile temperature rise. Adding this heat loss rate back to the enthalpy rate of the exiting air flow gives the enthalpy rate of the air entrained into the fume stack and is ultimately only a function of the thermopile temperature-rise. As a result, the fume stack is designed optimally to derive the sensible heat release rate from the thermopile temperature-rise.

The signal from the compensator can be used to correct the lag in the thermopile signal by using deviations from their steady-state ratio. To calibrate the appropriate correction, we set the panel irradiance at 51 kW/m^2, imposed a stepping function of the heat release rate into the fume stack, and recorded signals ***from the*** thermopile and compensator. Results are shown in Figure 4. A compensation formula given by

$$T_{cp} = T_p + 0.5\ (0.645\ T_p - T_c) \qquad (15)$$

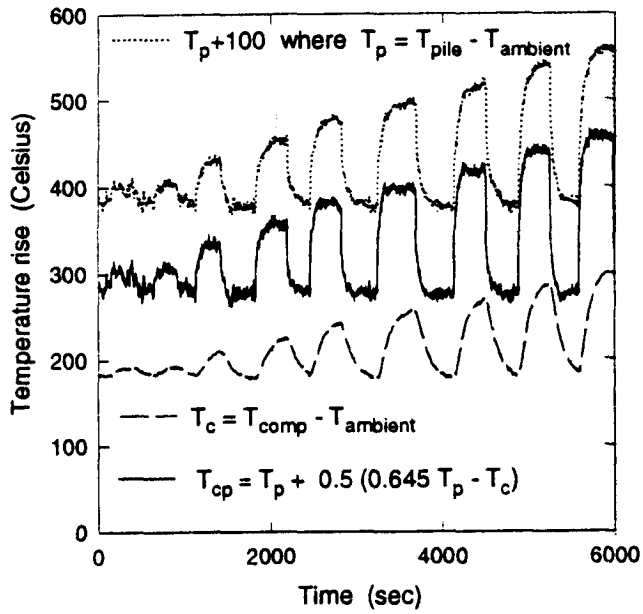

Figure 4 Compensation to thermopile temperature using fume temperature

was found adequate for flattening the peaks and valleys, as shown by the solid line in Figure 4, and yet retained steady-state values of the thermopile signal. This compensation formula was found applicable to other panel irradiance settings. In correlating data, we used nine levels of heat release rate. This is shown in Figure 5. Of significance is the open triangle data obtained with the gas panel burner turned off. The pyrometer sensed a small radiant reelection of methane flame by the gas panel burner and is included in the simple and invertible correlation,

$$T_{cp} = \frac{50\,\dot{H}^{0.8} + 11.5\,I_{50}}{1 + 0.021\,I_{50}} \tag{16}$$

Note that the correlation is not a smooth curve because the actual irradiance values were used in correlating the data, and the irradiances reported in Figure 5 are merely averaged values for the purposes of organizing the data. If the heat release rate. $\dot{H}$, is zero, the panel irradiance at 50 mm. I_{50}, will preheat the entrained air (the numerator term in equation 16) and affect air flow rate (the denominator term in equation 16) at entrance to the fume stack. As the heat release rate increases, its effect on heating and accelerating the entrained air is correlated by the power law correlation (the numerator term in equation 16). Since most of the flame is within the fume stack and not visible to the thermopiles because of the baffles, most radiant energy loss to

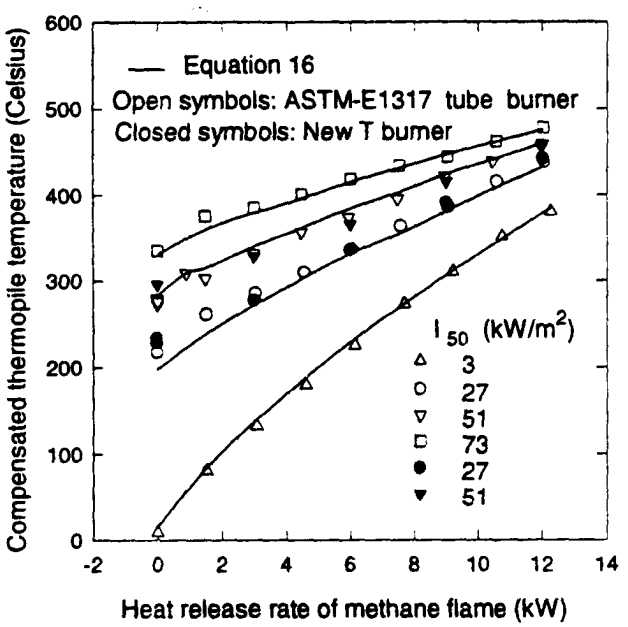

Figure 5 Correlation for the heat release rate using the methane calibration burner

the stack becomes recaptured by the entrained air flow. The error in heat release rate caused by radiant energy loss from the specimen will depend on how different the radiant emission of the methane flames is from that of the specimen. The T burner and the E-1317 tube burner gave equivalent calibration results.

Heat Release Rate of Douglas Fir Plywood. To calculate heat release rate using equation 16, our data acquisition system recorded the signals from the pyrometer, the thermocouple at ambient temperature the thermopile, and the compensator. These data were processed to provide heat flux at 50 mm, thermopile temperature-rise, and compensator temperature rise as a function of time. Equation 16 was inverted to obtain heat release rate as a function of I_{50}, T_p, and T_c and is plotted as function of time (Figure 6). A heat release rate divided by burning area during the transition to strip fire spreading at time 150 seconds is computed as 85 kW/m^2. In the corresponding Cone Calorimeter data on a vertical Douglas Fir plywood specimen with irradiance at 50 kW/m^2 and at 150 seconds, the heat release flux is 87.4 kW/m^2, which is about the same. Although the irradiance on the LIFT at the 370-mm location is about 40% that at the 50-mm location, thus implying a lower overall heat release flux, it is compensated by a peak heat release flux as high as 200 kW/m^2 at the 370-mm location. To more accurately calculate this effect, we are modifying Dietenberger's *(7)* Furniture Fire Model for our wood specimen in the LIFT setup.

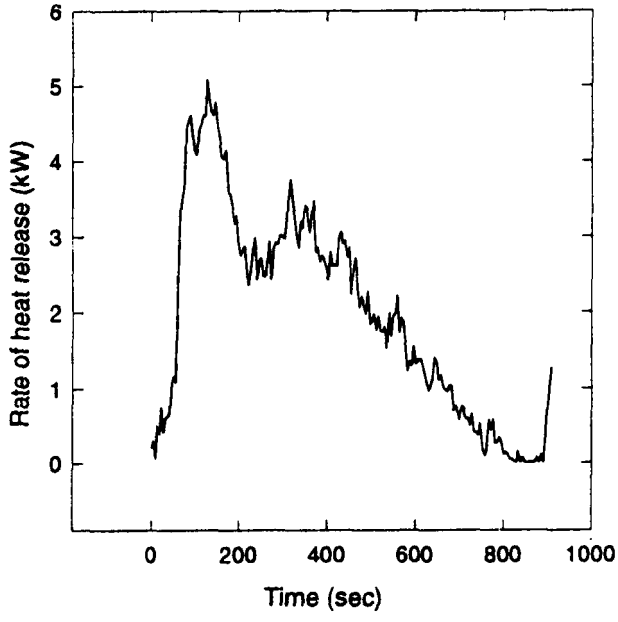

Figure 6 Heat release rate of DF plywood using FPL's thermopile method

Conclusions

Results of this research indicate that for studies of ignitability, surface emissivity and thickness of the specimen should be measured before testing. In addition, the irradiance profile and the convective heat transfer coefficient should be carefully calibrated and correlated. During testing, a thermal shutter should be used at high panel irradiances. **A** full range of achievable irradiances for piloted ignition is recommended for ignitability testing, because our empirical formula for materials of finite thickness cart be used to derive reasonable values for the ignition temperature. thermal diffusivity, and thermal conductivity. If we had used "nominal" values of emissivity, 0.88, and convective heat transfer coefficient, 0.015 kW/Km^2, and applied Janssens's correlation to our thickest plywood, the derived ignition temperature would have been 68°C greater than our value. Indeed, the same techniques developed in this work can be applied to the Cone Calorimeter or similar apparatus for ignitability. It is not surprising that the critical heat fluxes vary significantly among the different apparatuses, because convective cooling of the specimen is quite different.

If proposals to eliminate the preheating before lateral flame spreading are made part of E 1321, then there is a need to improve measurements of the lateral flame spread. **A** movable indicator linked to a potentiometer has been tested and proved adequate. An appropriate flame spread formula has been used that accounts for three transitions of heat transfer behavior occurring on a typical specimen during flame spreading. These transitions are thermally thick to thin transition, convective cooling

to flame heating transition, and the transition to the spread of flame limit. Flame spread in various directions can benefit from this analysis. These new procedures for analyzing ignitability and flame spread data obtained with the LIFT apparatus should also result in a major revision of the E-1321 standard (and similar standards) and an increased use of the LIFT apparatus. Further studies that include measurements of the flame front properties should add insight to the flame spread mathematical formulation.

A new method to compensate the thermopile signal for the fume stack thermal inertia and a new calibration of the heat release rate as a function of compensated thermopile signal and panel irradiance are significant improvements for E-1317. The methane "T" burner similar to that in E-906 is a convenient substitute for E-1317 methane line burner. The methane flame does not affect convective heat transfer coefficients over instrumented calibration plugs located at 50 mm or further from the flame. Thus, simultaneous calibrations for heat release rates and convective heat transfer coefficients have been achieved and can be adopted for greater efficiency.

Nomenclature

Bi	Biot number (equation 6)
C	Factor for flame-edge buoyant velocity
Fo	Fourier number (equation 5)
g	Local gravitational acceleration (m/s^2)
h_c	Convective transfer coefficient (kW/Km^2)
h_{ig}	Linearized transfer coefficient (kW/Km^2)
$\dot{H}$	Heat release rate (kW)
I_{50}	Irradiance at 50 mm position (kW/m^2)
T	Temperature (K)
T	Normalized temperature
q	Surface heat flux (kW/m^2)
V	Lateral velocity (m/s)
x	Lateral position (m)
α	Thermal diffusivity (m^2/s)
δ	Thickness (m)
δ^*	Transitional thickness (m)
λ	Thermal conductivity (kW/Km)
ε_s	Surface emissivity
ρC_p	Heat capacitance (kJ/Km^3)
σ	Stefan-Boltzmann constant (5.67e-11 kW/K^{4}m^2)

subscripts

a	Entrained air
c	Fume stack thermocouple
cf	Flame edge convection
cp	Compensated thermopile
e	Surface preheating
f	Lateral flame edge
$f\infty$	Infinitely thick material
ig	Material surface at ignition
p	Thermopile
-	No-subscript for material
Thick	Thermally thick material
Thin	Thermally thin material

Acknowledgements

The author is indebted to Dr. Robert White for his support and guidance for this internal study and to Anne Fuller for acquiring data with the LIFT apparatus.

Literature Cited

1. ASTM E 1321-90. Standard Test Method for Determining Material Ignition and Flame Spread Properties. American Society for Testing and Materials, Philadelphia (1990).
2. ASTM E 1317-90. Standard Test Method for Flammability of Marine Surface Finishes. American Society for Testing and Materials, Philadelphia (1990).
3. ISO 5660. International Standard for Fire Tests - Reaction to Fire - Rate of Heat Release from Building Products. International Organization for Standardization, Geneva (1991).
4. Whitely, R.H., Short Communication - Some Comments on the Measurement of Ignitability and on the Calculation of 'Critical Heat Flux'. *Fire Safety Journal* **21** (1993) 177-183.
5. Shields, T.J.,Silcock G.W., and Murray, J.J., The Effects of Geometry and Ignition Mode on Ignition Times Obtained Using a Cone Calorimeter and ISO Ignitability Apparatus. *Fire and Materials* **17** (1993) 25-32.
6. Janssens, M., Fundamental Thermophysical Characteristics of Wood and their Role in Enclosure Fire Growth. Ph.D. Thesis, University of Gent, Belgium, November 1991.
7. Dietenberger, M., Chapter 13: Upholstered Furniture - Detailed Model. Heat Release in Fire, V. Babrauskas and S. Grayson, eds., Elsevier Science Publishers Ltd., 1992.
8. Dietenberger, M.A., Piloted Ignition and Flame Spread on Composite Solid Fuels in Extreme Environments. Ph.D. Thesis, University of Dayton, Dayton Ohio, December 1991.

RECEIVED December 23, 1994